GLUT-1/PKM2 loop dysregulation in patients with non-ST-segment elevation myocardial infarction promotes metainflammation

Francesco Canonico [1], Daniela Pedicino [1]*, Anna Severino[2], Ramona Vinci [1,2], Davide Flego[2], Eugenia Pisano[1], Alessia d'Aiello[2], Pellegrino Ciampi[2], Myriana Ponzo [2], Alice Bonanni [1,2], Astrid De Ciutiis[2], Sara Russo[2], Marianna Di Sario [2], Giulia Angelini[1,2], Piotr Szczepaniak[3,4], Alfonso Baldi[5], Boguslaw Kapelak[6], Karol Wierzbicki[6], Rocco A. Montone [1], Domenico D'Amario [1], Massimo Massetti[1,2], Tomasz J. Guzik [3,4], Filippo Crea [1,2]†, and Giovanna Liuzzo [1,2]†

[1]Department of Cardiovascular Sciences, Fondazione Policlinico A. Gemelli, IRCCS, Largo A. Gemelli 8, 00168 Rome, Italy; [2]Department of Cardiovascular and Pneumological Sciences, Catholic University of Sacred Heart, Rome, Italy; [3]Institute of Cardiovascular and Medical Sciences, University of Glasgow, Glasgow, UK; [4]Department of Internal and Agricultural Medicine, Jagiellonian University, Collegium Medicum, Krakow, Poland; [5]Department of Environmental, Biological and Pharmaceutical Sciences and Technologies, University of Campania 'Luigi Vanvitelli', Caserta, Italy; and [6]Department of Cardiovascular Surgery and Transplantology, Jagiellonian University, John Paul II Hospital, Krakow, Poland

Aims	The functional capacity of the immune cells is strongly dependent on their metabolic state and inflammatory responses are characterized by a greater use of glucose in immune cells. This study is aimed to establish the role of glucose metabolism and its players [glucose transporter 1 (GLUT-1) and pyruvate kinase isozyme M2 (PKM2)] in the dysregulation of adaptive immunity and inflammation observed in patients with non-ST-segment elevation myocardial infarction (NSTEMI).
Methods and results	We enrolled 248 patients allocated to three groups: NSTEMI patients, chronic coronary syndromes (CCS) patients, healthy subjects (HSs). NSTEMI patients showed higher expression of GLUT-1 and an enhanced glucose uptake in T cells when compared with CCS patients ($P < 0.0001$; $P = 0.0101$, respectively) and HSs ($P = 0.0071$; $P = 0.0122$, respectively). PKM2 had a prevalent nuclear localization in T lymphocytes in NSTEMI ($P = 0.0005$ for nuclear vs. cytoplasm localization), while in CCS and HS, it was equally distributed in both compartments. In addition, the nuclear fraction of PKM2 was significantly higher in NSTEMI compared with HS ($P = 0.0023$). In NSTEMI patients, treatment with Shikonin and Fasentin, which inhibits PKM2 enzyme activity and GLUT-1-mediated glucose internalization, respectively, led to a significant reduction in GLUT-1 expression along with the down-regulation of pro-inflammatory cytokine expression.
Conclusion	NSTEMI patients exhibit dysregulation of the GLUT-1/PKM2 metabolic loop characterized by nuclear translocation of PKM2, where it acts as a transcription regulator of pro-inflammatory genes. This detrimental loop might represent a new therapeutic target for personalized medicine.

---

* Corresponding author. Tel: +39 06 30154187, fax: +06 3055 535, E-mail: daniela.pedicino@policlinicogemelli.it; danialla@gmail.com

† These authors contributed equally to this work.

Graphical Abstract
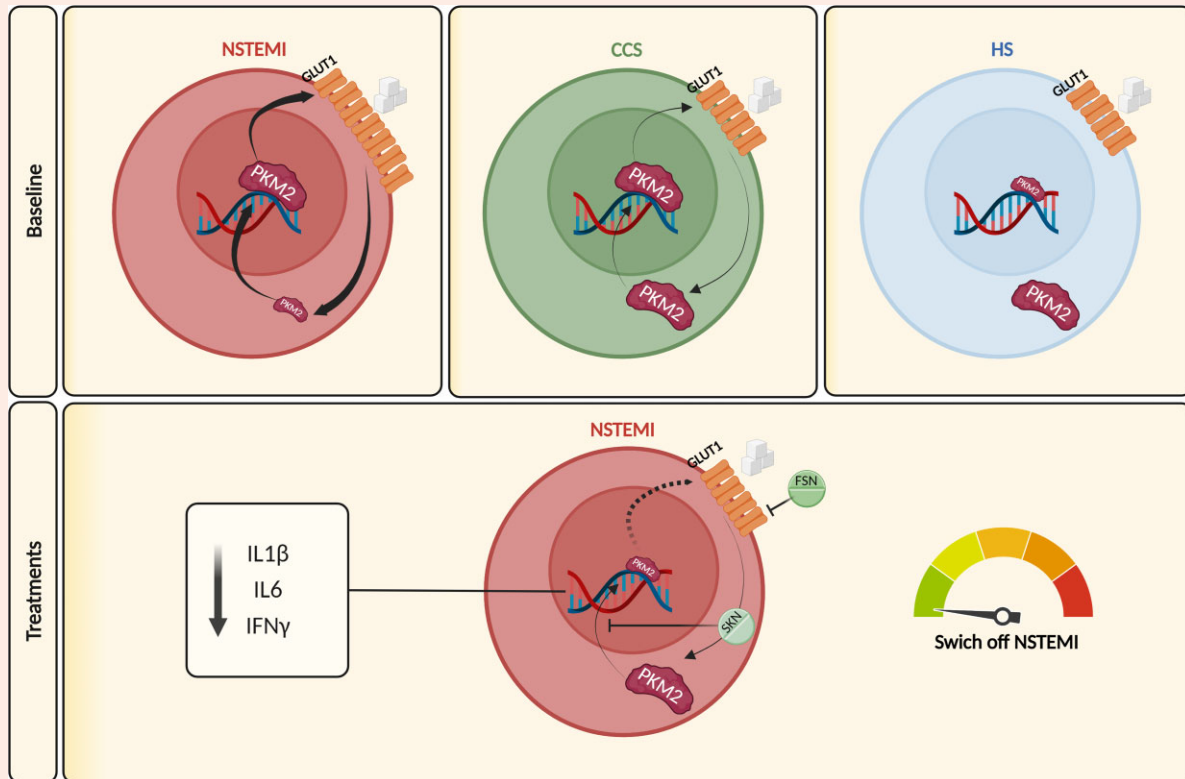
GLUT-1/PKM2 metabolic loop and inflammatory pathways. PKM2 plays a central role in the modulation of the metabolic and inflammatory state. Our data showed aberrant localization of PKM2, in patients with NSTEMI, promoting enhanced GLUT-1 expression and glucose metabolism that shifts adaptive immunity towards a pro-inflammatory profile. The functional effects of the disruption of the metabolic loop GLUT-1/PKM2, through treatment with SKN and FSN in NSTEMI patients, led to a reduction of the pro-inflammatory profile and a modulation of the factors involved in lipid metabolism, contributing to the re-establishment of a physiological phenotype. Conversely, the treatment of HS with OLI, an inhibitor of oxidative phosphorylation, promotes GLUT-1 enhancement and a PKM2 dependent pro-inflammatory profile (not shown). Therefore, the evaluation of the immuno-metabolic profile could help to stratify NSTEMI patients and allow the identification of new therapeutic targets in the perspective of a personalized medicine approach [Created with BioRender.com]. ApoA1, apolipoprotein A1; CHI3L1, chitinase-3 like-1; FSN, fasentin; GLUT-1, glucose transporter 1; IL-6, interleukin 6; MPO, myeloperoxidase; PDGF, platelet-derived growth factor; PKM2, pyruvate kinase isozyme M2; RBP4, retinol-binding protein 4; SKN, shikonin.

1. Introduction

Substantial evidence supports a pivotal role for local and systemic inflammation in the pathogenesis of coronary artery disease (CAD). In particular, in the past few years, our and other research laboratories have demonstrated that dysregulation of adaptive immunity plays a key role in acute coronary syndrome (ACS).[1–4] Indeed, patients with ACS are characterized by an immune imbalance towards pro-inflammatory Th-lymphocyte response and a reduced frequency of regulatory T cells (Treg) with compromised functional suppressive properties, which might be involved in specific plaque instability mechanisms.[5]

Emerging data indicate that cellular metabolism regulates immune cell functions and differentiation in response to local changes of microenvironment. The molecular signalling linking cell metabolism to the immune response is not yet been fully understood.[6–8] During a physiological immune response, T cells rapidly shift from resting (naïve and memory T cells) to activated states (effector T cells), with a dramatic increase of glucose metabolism. Enhanced glycolysis in CD4+ T cells is associated with post-transcriptional regulation of specific cellular functions and with abnormal immune responses. Recent developments in the immune-metabolism field focused on its role in cancer and in different inflammatory conditions such as autoimmune disorders, diabetes, obesity, as well as atherosclerosis. However, the potential impact of an altered immune cell metabolism as a clinical marker and therapeutic target in cardiovascular disease remains unclear.[9,10]

Glucose transporters (GLUTs) are potentially the key metabolic targets with relevance to regulation of immune responses. GLUT-1 is the main facilitative trans-membrane GLUT which plays a role in T-cell activation and differentiation.[11] It is expressed at low levels on the surface of resting T cells and it is up-regulated upon T-cell activation. T cells have a cytoplasmic pool of GLUT-1 whose translocation to the cell surface is responsible for increased glucose uptake after activation. The release of glucose into the cytoplasm occurs after the conformational changes of GLUT-1 promoted by substrate binding.[11]

The development of drugs that limit cellular glucose uptake, with a consequent decrease in glycolysis, is of growing interest, and several classes of

compounds that inhibit GLUTs and glucose absorption might be considered to this end.[12–14] Another potential metabolic target is the pyruvate kinase isozyme M2 (PKM2), the final rate-limiting enzyme in glycolysis that catalyses the conversion of phosphoenolpyruvate to pyruvate. Recently, a role has emerged for PKM2 that goes beyond glycolysis regulation, bridging metabolism, and differentiation both in cells of innate and adaptive immunity, and PKM2 intracellular localization strongly influences this function. Indeed, the nuclear dimeric form acts as a transcription regulator of pro-inflammatory genes, while, in the cytoplasmic tetrameric form, PKM2 exploits its well-known enzymatic functions in glycolysis. PKM2 activity can be influenced by many allosteric effectors and post-translational modifications that change its conformation.[15] A recent study highlighted the GLUT-1/PKM2 linkage in the glycolytic metabolic cycle; in particular, the intra-nuclear dimeric form of PKM2 promotes the protein expression of GLUT-1, consequently affecting glucose uptake and energetic cell metabolism.[16] Shikonin (SKN) selectively inhibits PKM2 and the glycolytic rate in cancer cell lines, highlighting its potential in future clinical applications.[17–20] Another PKM2 potential regulator is jumonji C (jmjC) domain-containing isotype 8 protein (JMJD8), a member of the jmjC domain-only subgroup in jumonji family. JmjC domain-containing proteins operate as histone demethylases, which modify chromatin accessibility and, accordingly, regulate gene transcription.[21] Members of this family are involved in cell proliferation and differentiation through the regulation of various signalling pathways. Recently, a role for JMJD8 has emerged as a positive regulator of tumour necrosis factor–induced nuclear factor kappa-light-chain-enhancer of activated B cells signalling. Although JMJD8 usually presents a nuclear localization, the latest studies have shown that JMJD8 controls angiogenesis and cellular metabolism by interacting with PKM2 in the cytoplasm of endothelial cells.[22]

The aim of the present study was to investigate the modulation of glucose metabolism in T-cell dysregulation of patients with non-ST-elevation myocardial infarction (NSTEMI). To achieve this, we focused on GLUT-1 expression, glucose uptake, PKM2, and JMJD8 function in T lymphocytes in CAD patients with NSTEMI.

2. Methods

2.1 Study population

In the present study, the total study population size consisted of 248 subjects (see Supplementary material online, Table S1). We enrolled:

- 107 patients admitted to our coronary care unit with a diagnosis of NSTEMI. NSTEMI patients were defined with the detection of the rise and fall of cardiac Troponin I together with symptoms and/or signs of myocardial ischaemia (angina, ischaemic ST changes), and angiographically confirmed CAD at coronary angiography.[23]
- 105 chronic coronary syndrome (CCS) patients, with angiographically confirmed CAD, no previous ACS, and no overt ischaemic episodes during the previous 48 h.[24]
- 36 healthy subjects (HSs) as healthy control group.

No patient selection was made based on blood glucose values. The study has been approved by the Ethics Committee of the Fondazione Policlinico Universitario A. Gemelli-IRCCS, Catholic University of Rome (Approval No. 36077/19-ID 2747).

The authors declare that their study complies with the Declaration of Helsinki, that the locally appointed ethics committee has approved the research protocol, and that informed consent has been obtained from the subjects (or their legally authorized representative).

2.2 Study population of coronary artery samples

The total size of the study population consisted of 10 patients with ($n = 4$; CAD) and without ($n = 6$; no-CAD) previous myocardial infarction. Written informed consent was obtained from all patients. The study was approved by the local ethics committee of the Jagiellonian University (Approval No. 1072.6120.162.2019). Clinical data including major risk factors for cardiovascular diseases were recorded before surgery. The baseline patient characteristics are presented in Supplementary material online, Table S2.

2.3 Peripheral blood mononuclear cell stimulations

Peripheral blood mononuclear cells (PBMCs) were isolated from whole-blood samples by standard gradient centrifugation over Ficoll–Hypaque (GE Healthcare Bio-Sciences, Piscataway, NJ, USA). PBMC stimulation was performed for 48 h with anti-CD3 monoclonal antibody (mAb) and CD28 mAb; goat anti-mouse IgG (BD Bioscience, Mountain View, CA, USA) was added for induction of cross-linking.[25]

For glucose uptake, cells were transferred in glucose-free medium and 2-NBDG {2-deoxy-2-[(7-nitro-2,1,3-benzoxadiazol-4-yl)amino]-D-glucose}, and a fluorescently labelled 2-deoxyglucose, was added. Analysis was performed using a 2-NBDG glucose uptake kit from Cayman Chemical (Ann Arbor, MI, USA).

Inhibition of PKM2 and GLUT-1 was obtained by adding, respectively, 50 µM SKN (Tocris Bioscience, Bio-techne, Minneapolis, MN, USA) for 6 h[26] and 25 µM Fasentin (FSN)[27] (Santa Cruz Biotechnology, Dallas, TX, USA) for 6 h, in CD3/CD28-treated PBMCs.

To mimic a condition of mitochondrial stress by inhibition of ATP synthase, CD3/CD28-stimulated PBMCs of HS were treated with 1 µM Oligomycin (OLI)[28,29] for 1 h (Santa Cruz Biotechnology).

2.4 Flow-cytometry analysis

For surface cell markers characterization, PBMCs were incubated with fluorochrome-conjugated mAbs anti-CD4 PE-Cy5 (Beckman Coulter, Brea, CA, USA), and GLUT-1 PE (R&D, Minneapolis, MN, USA). For glucose internalization analysis, PBMCs were stained with anti-CD4 PE-Cy5 and 2-NBDG glucose uptake kit from Cayman Chemical was used.

For intracellular protein staining, cells were fixed and permeabilized with Fix/Perm buffer (Thermo Fisher Scientific, Waltham, MA, USA) and incubated with anti-PKM2 PE (Abcam, Cambridge, UK) and anti-JMJD8 FITC (Aviva Systems Biology, San Diego, CA, USA). Unstained cells were used as negative control. The gating strategies used for the flow-cytometry evaluations of PKM2, glucose uptake, and GLUT-1 in CD4$^+$ T cells are summarized in Supplementary material online, Figure S1.

No cell viability assays using fluorescent methods were performed. As previously reported, the combination of forward scatter (FSC) and side-ward scatter (SSC) provides a tool, which although not as precise as the fluorescence methods, still give valuable results in many assays. Therefore, we identified apoptotic or dying cells without any staining by FSC and SSC parameters only considering the morphology.

Flow-cytometry analysis was conducted with FC 500 (Beckman Coulter) and data were analysed with Kaluza software (Beckman Coulter) considering the median fluorescence intensity (MFI). At least 50 000 events were acquired.

2.5 RNA extraction and real-time polymerase chain reaction analysis

Total RNA was extracted from PBMCs, using RNeasy Plus Mini Kit (Qiagen, Hilden, Germany) according to the instructions provided by the company and then reverse transcribed into cDNA using iScript RT (Bio-Rad, Hercules, CA, USA). To assess PKM2 levels, we set up a duplex Taqman assay including PrimePCR™ Probe (Hex) Assay: PKM2 and PrimePCR™ Probe (Cy5) Assay: β2 microglobulin (B2M; Bio-Rad). To evaluate the inflammatory gene expression, interleukin (IL)-1β and IL-6 primer sequences were used as described,[15] while, interferon gamma (IFNγ) primer sequences were used as follows:

IFNγ forward primer: 5′-GCTCTGCATCGTTTTGGGTTC-3′
IFNγ reverse primer: 5′-TTTTCTGTCACTCTCCTCTTTCC-3′

Real-time polymerase chain reaction was conducted in the CFX96 Touch (Bio-Rad). The expression level of PKM2 was normalized with B2M and the relative gene expression was obtained using the 2-ΔΔCT method.

2.6 Pyruvate kinase enzyme activity
Lysate of unstimulated PBMCs was used for the pyruvate kinase enzyme activity test (Abcam) following the manufacturer's instructions. Zero standard readings were subtracted from the standards. The pyruvate standard curve was plotted. A1 reading was measured at fluorescence Ex/Em = 535/587 nm at T1. A2 reading was measured at T2 after incubating the reaction at 25°C for 10 min, protected from light. The ΔA (A2 − A1) to the standard curve was applied to get nmol of pyruvate generated between T1 and T2 by PK in the reaction wells. Fluorescent measurement was obtained using a Varioskan™ LUX multimode microplate reader (Thermo Fisher Scientific).

2.7 Immunofluorescence and confocal microscopy
PBMCs stimulated with anti-CD3/CD28, treated with or without SKN, FSN, and OLI, were fixed with 10% formalin. After 24 h, cells were permeabilized with 0.3% Triton X and 0.3% bovine serum albumin and stained with primary antibodies anti-PKM2 (Abcam) and anti-JMJD8 (Santa Cruz Biotechnology) overnight at 4°C, followed by the application of the secondary antibody: Alexa Fluor 488 (anti-mouse; Abcam) and Alexa Fluor 546 (anti-rabbit), respectively; 4′,6-diaminophenyl-indole (DAPI) was used for nucleus staining. Finally, cells were washed and mounted with ProLong® Gold Antifade Mountant (Thermo Fisher Scientific) and stored in dark at 4°C until imaging. Confocal images were obtained with a Nikon A1 MP confocal scanning system connected to an Eclipse T-i microscope with a 60× objective plus further 3× magnification.

For confocal microscopy analysis, 5–7 images were collected for each treatment, containing $n \geq 10$ cells and analysed by mean fluorescence or Manders' test,[30] whose coefficient is the co-localization fraction directly proportional to the amount of fluorescence, in the co-localized objects, in each colour channel of the dual-channel image. Confocal microscopy analyses were performed with ImageJ Fiji (National Institute of Health, Bethesda, MD, USA).

2.8 Proteome profile
Proteome profile of the supernatants resulting from PBMC stimulation of NSTEMI patients, with SKN ($n = 7$) and FSN ($n = 7$) was evaluated using the Proteome Profiler Assay Human XL Cytokine Array Kit (R&D Systems, Minneapolis, MN, USA) as suggested by the manufacturer's instructions. Densitometry analysis was performed with Image Lab 6.2 (Bio-Rad).

2.9 Human coronary arteries sampling
Tissue samples of coronary arteries were obtained from the Department of Cardiovascular Surgery and Transplantology of the John Paul II Hospital in Krakow (Poland) during heart transplantation. The coronary arteries were immediately transferred to ice-cold Hank's Balanced Salt Solution (Gibco; Thermo Fisher Scientific) buffer and were maintained at 4°C. Surrounding tissues were delicately separated using microsurgical instruments and a microscope. Samples used in the present study included left anterior descending or circumflex human coronary arteries (HCAs).

2.10 HCA immunohistochemistry
Cleared HCA samples were immediately snap frozen and embedded in Tissue-Tek OCT, and stored at −80°C. Samples were then cut into a series of consecutive 8 μm sections. For histological analysis, sections were fixed in paraformaldehyde for 5 min, then haematoxylin and eosin staining was performed. For immunohistochemistry, consecutive sections were fixed in paraformaldehyde for 5 min, then washed in phosphate-buffered saline.

Phosphate-buffered saline was used for all the subsequent washes and for antibody dilutions. Antibodies anti-CD4 (Abcam), anti-PKM2 (Abcam), and anti-GLUT-1 (Abcam) were incubated for 1 h at room temperature at a dilution of 1:100, then with diluted anti-polyvalent Ultratek horseradish peroxidase antibody conjugated with streptavidin for 1 h. All the slides were finally processed by the avidin–biotin complex method for 30 min at room temperature. 3,3′-Diaminobenzidine (Histo-Line Laboratories, Milan, Italy) was used as the final chromogen and haematoxylin was used as the nuclear counterstain. All samples were processed under the same conditions. The presence of lymphocytes was determined by analysis of both haematoxylin and eosin stainings.

2.11 Statistical analysis
Data were described as mean ± standard deviation (SD) or median with interquartile range (IQR), based on their distribution. For comparisons between groups, we used the Mann–Whitney test, if the results did not pass the test for a normal distribution; otherwise, we used a parametric test; for categorical variables, a χ^2 test or a Fisher's exact test was used, as appropriate. For intragroup analysis, we used one-way analysis of variance (ANOVA) nonparametric test, Kruskal–Wallis test with Dunn's multiple comparison test or two-way ANOVA with Sidak's multiple comparisons test, as appropriate. A *P*-value <0.05 was considered statistically significant. Statistical analysis was performed with GraphPad Prism version 8.0.2 (GraphPad Software, San Diego, CA, USA).

Multivariate regression analysis, with glucose uptake, GLUT-1, and PKM2 as dependent variables, was run on data of the study population after adjusting for pharmacological treatments.

3. Results
Demographic and clinical characteristics of the study population are presented in Supplementary material online, *Table S1*.

3.1 GLUT-1 expression and glucose uptake
In a quiescent state, CD4$^+$ T cells express the surface glucose transporter GLUT-1 at very low levels. We therefore evaluated GLUT-1 expression and glucose uptake after 48 h lymphocyte stimulation with anti-CD3 and anti-CD28 cross-link. In these conditions, T cells from NSTEMI patients ($n = 28$) showed a significantly higher GLUT-1 expression and glucose internalization, when compared with CCS ($n = 31$) and with HS ($n = 8$) [(GLUT-1 MFI, mean ± SD): NSTEMI 4.44 ± 1.46 vs. CCS 2.98 ± 1.10; $P < 0.0001$; NSTEMI vs. HS 2.92 ± 0.07; $P = 0.0071$] [Glucose uptake (intended as the MFI of the 2-NBDG probe, median and IQR): NSTEMI 4.72 (3.17–5.70) vs. CCS 3.31 (2.37–3.51); $P = 0.0101$; NSTEMI 4.72 (3.17–5.70) vs. HS 2.77 (2.70–3.20); $P = 0.0122$] (*Figure 1A and B*).
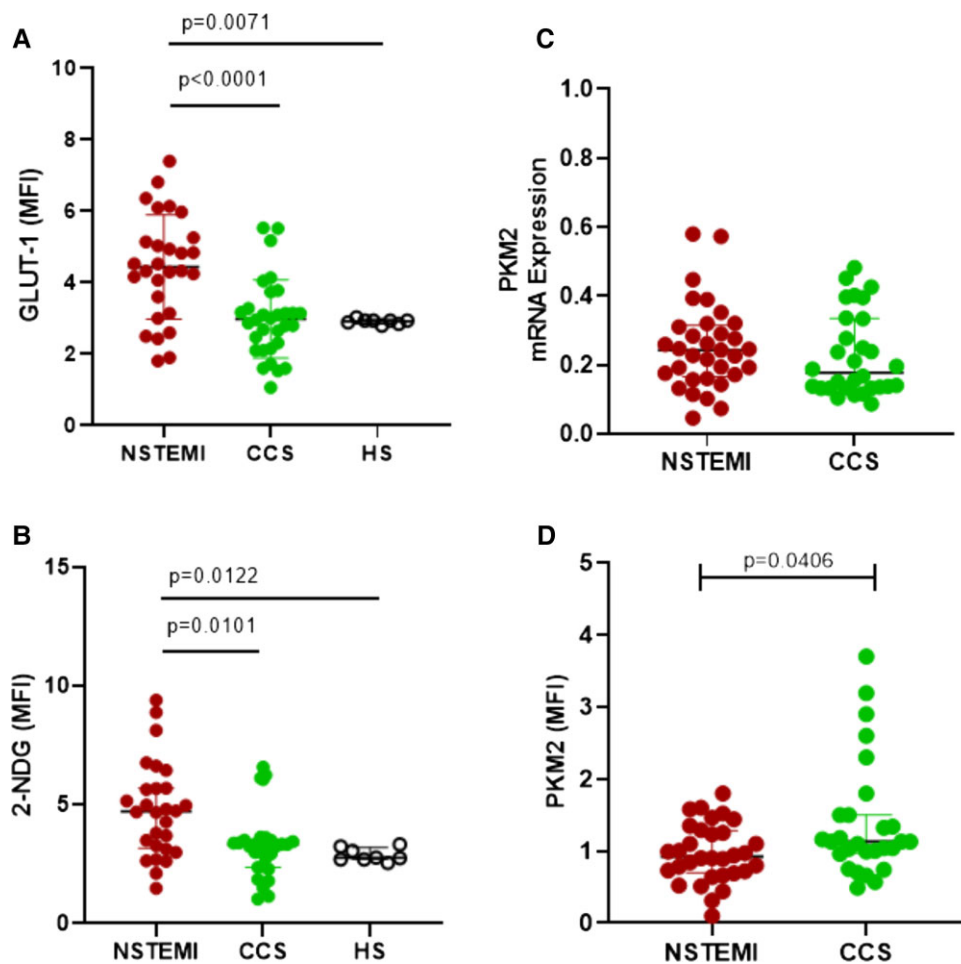
3.2 PKM2 expression
To better understand the underlying mechanism of the dysregulation of GLUT-1 in NSTEMI patients, we evaluated PKM2 expression, since it is an activator of GLUT-1 with an emerging role in metabolism-inflammation cross-talk. PKM2 mRNA levels in PBMCs showed no difference between NSTEMI ($n = 33$) and CCS ($n = 30$) patients. At flow-cytometry, PKM2 protein expression in CD4$^+$ T cells was higher in CCS patients ($n = 30$) compared with NSTEMI ($n = 33$) patients [PKM2 MFI, median and IQR: 1.13 (0.97–1.50) vs. 0.92 (0.70–1.28); $P = 0.0406$] (*Figure 1C and D*).

A further analysis, stratifying patients by fasting blood glucose values (>110 mg/dL, the cut-off to define fasting hyperglycaemia[31] or <110 mg/dL), revealed that PKM2 mRNA and protein expression was related to blood glucose levels only in CCS and not in NSTEMI patients, as shown in Supplementary material online, Supplementary material and *Figures S2 and S3*.

On the other hand, we found an increased enzymatic activity of PKM2 in PBMCs of NSTEMI ($n = 13$) patients compared with CCS patients ($n = 14$), suggesting an enhanced glycolytic rate [PKM2 activity (mU/mL), mean ± SD: NSTEMI 309.9 ± 167.2 vs. CCS 168.9 ± 122.7, $P = 0.0189$] (see Supplementary material online, *Figure S4*).

Figure 1 GLUT-1 and PKM2 dependent glucose metabolism in CD4$^+$ T cells and PBMCs. (A) GLUT-1 protein level and (B) glucose uptake in NSTEMI, CCS, and HS; (C) PKM2 mRNA expression and (D) PKM2 protein expression in NSTEMI and CCS patients. In (A), the data were described as mean ± standard deviation, based on their distribution. For intragroup analysis, we used one-way ANOVA with Tukey's multiple comparison test. In (B), the data were described as median with interquartile range, based on their distribution. For intragroup analysis, we used one-way ANOVA nonparametric test, Kruskal–Wallis test with Dunn's multiple comparison test. In (C) and (D), the data were described as median with interquartile range, based on their distribution. For comparisons between groups, we used the Mann–Whitney test. 2-NDG, 2-deoxy-2-[(7-nitro-2,1,3-benzoxadiazol-4-yl)amino]-D-glucose; GLUT-1, glucose transporter 1; MFI, median fluorescence intensity; PKM2, pyruvate kinase isozyme M2; PBMC, peripheral blood mononuclear cell.

3.3 Aberrant PKM2 intra-nuclear localization in NSTEMI patients

Since PKM2 intracellular localization strongly influences its function, we evaluated its nuclear and cytoplasmic fraction in PBMCs. Confocal fluorescence microscopy revealed that PKM2 was localized mainly in the nucleus in NSTEMI ($n = 12$) [MFI, median and IQR: intra (i)NSTEMI 3.7×10^4 (2.3×10^4–9.1×10^4) vs. extra (e)NSTEMI 0.7×10^4 (0.5×10^4–2.8×10^4); $P = 0.0005$], while CCS ($n = 5$) patients and HS ($n = 8$) showed a homogeneous distribution of PKM2 between the two compartments. Interestingly, the nuclear fraction of PKM2 was significantly higher in NSTEMI compared with HS (Kruskal–Wallis test $P = 0.0035$; Dunn's multiple comparison (i)NSTEMI vs. iHS $P = 0.0023$; *Figure 2A*). A representative staining is showed in *Figure 2B*.

A putative regulator of PKM2, JMJD8 was also evaluated in the same patients. JMJD8 expression in CD4$^+$ T cells of NSTEMI patients ($n = 12$) was higher than in CCS patients ($n = 22$; MFI, mean ± SD: 4.01 ± 0.71 vs. 3.33 ± 0.67; $P = 0.0138$; see Supplementary material online, *Figure S5A*). However, as depicted in the Supplementary material online, *Figure S5B–E*, NSTEMI patients showed a lower nuclear localization of JMJD8 in PBMCs [two-way ANOVA $P = 0.0069$; Manders' tM2, iNSTEMI vs. eNSTEMI

median and IQR: 1.0×10^4 (0.8×10^4–2.5×10^4) vs. 5.3×10^4 (2.6×10^4–10.1×10^4); $P = 0.0036$], a lower PKM2/JMJD8 intra-nuclear co-localization [Manders' tM2, median and IQR: 0.59 (0.47–0.62) vs. 0.70 (0.69–0.78); $P = 0.0079$], and a higher PKM2/JMJD8 extra-nuclear co-localization [Manders' tM2, median and IQR: 0.45 (0.36–0.53) vs. 0.30 (0.23–0.32); $P = 0.0079$] when compared with CCS patients.

Overall these findings suggested a potential role of JMJD8 in the nuclear translocation of PKM2 in the NSTEMI patients.

3.4 Shikonin and Fasentin treatment reduces the intra-nuclear translocation of PKM2, GLUT-1 protein expression, and transcription of pro-inflammatory genes in NSTEMI patients

To confirm the role of PKM2 on GLUT-1 expression, we treated PBMCs of NSTEMI patients with SKN and FSN that inhibit PKM2 enzyme activity and GLUT-1-mediated glucose internalization, respectively.
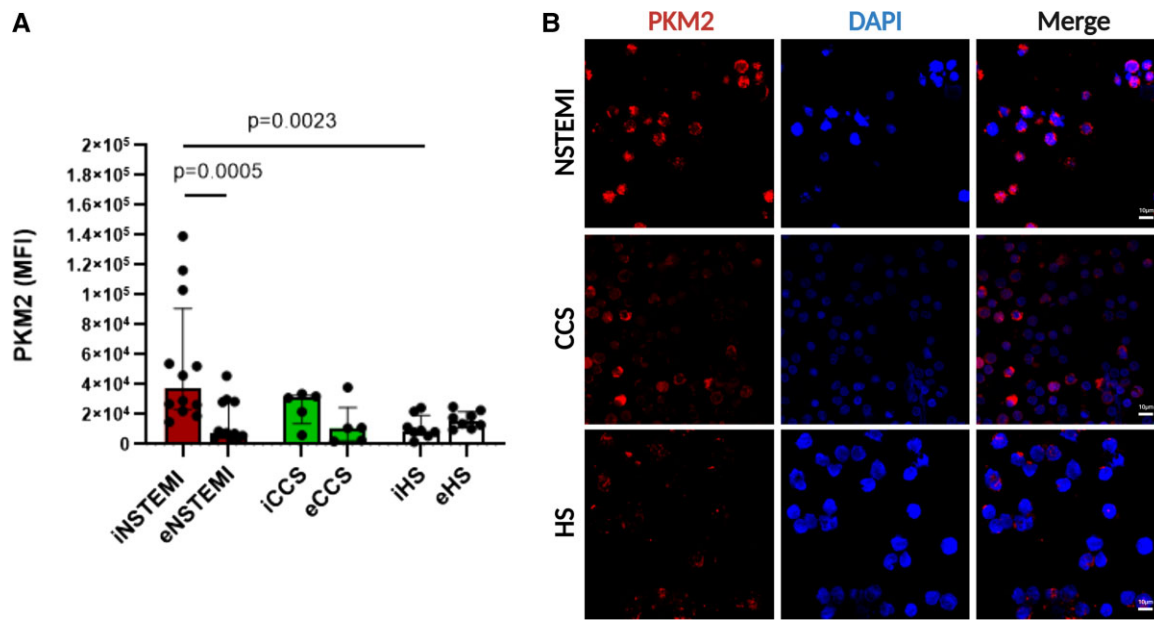
Figure 2 Intracellular localization of PKM2 in NSTEMI, CCS, and HS. (*A*) Intra- and extra-nuclear PKM2 fluorescence (MFI) in NSTEMI, CCS, and H; (*B*) Representative immunofluorescence confocal images of PKM2 in PBMCs; PKM2 = red fluorescence, nuclei = DAPI; scale bar: 10 μm for all images. In (*A*), the data were described as median with interquartile range, based on their distribution. For intragroup analysis, we used one-way ANOVA nonparametric test, Kruskal–Wallis test with Dunn's multiple comparison test. CCS, chronic coronary syndromes; (e), extra-nuclear; HS, healthy subject; (i), intra-nuclear; MFI, median fluorescence intensity; NSTEMI, non-ST-elevation myocardial infarction; PKM2, pyruvate kinase isozyme M2; PBMC, peripheral blood mono-nuclear cell.

We found that both treatments reduced the intra-nuclear translocation of PKM2 [Manders' tM2, mean ± SD: untreated vs. SKN (*n* = 8) 0.65 ± 0.12 vs. 0.44 ± 0.14, *P* < 0.0001; untreated vs. FSN (*n* = 8) 0.65 ± 0.12 vs. 0.37 ± 0.19, *P* = 0.0005; *Figure 3A–C*] and the expression of GLUT-1 on the cell surface [MFI, mean ± SD: untreated vs. SKN (*n* = 12) 4.439 ± 0.86 vs. 4.136 ± 0.82, *P* < 0.0001; untreated vs. FSN (*n* = 12) 4.439 ± 0.86 vs. 4.210 ± 0.88; *P* = 0.0117] breaking the PKM2 dependent metabolic loop (*Figure 3D and E*).

Moreover, both treatments led to a decrease of the mRNA levels of inflammatory genes directly related to T-cell activation such as IL-1β [untreated vs. SKN, median and IQR: 1.006 (0.91–1.55) vs. 0.472 (0.25–1.16), *P* = 0.0313; untreated vs. FSN 0.2337 (0.06–0.33); *P* = 0.0313]; IL-6 [untreated vs. SKN, mean ± SD: 0.9740 ± 0.63 vs. 0.5708 ± 0.42; *P* = 0.0300; untreated vs. FSN 0.4050 ± 0.29; *P* = 0.0214]; and IFNγ [untreated vs. SKN, median and IQR: 1.006 (0.83–1.70) vs. 0.7918 (0.47–1.20); *P* = 0.0625; untreated vs. FSN 0.2362 (0.18–0.47); *P* = 0.0313] (*Figure 3F*).

The proteome profile of stimulated PBMC supernatants following inhibition of PKM2 nuclear translocation and of GLUT-1-related glucose uptake revealed a significant reduction of pro-inflammatory mediators such as IL-6 (untreated vs. SKN *P* < 0.0001; untreated vs. FSN *P* < 0.0001), chitinase-3 like 1 (CHI3L1; untreated vs. FSN *P* = 0.024), myelo-peroxydase (MPO; untreated vs. FSN *P* = 0.050), IL-1 receptor antagonist (IL-1RA; untreated vs. FSN *P* = 0.046) with the latter three decreasing significantly only after treatment with FSN. In addition, we found an increased level of apolipoprotein A1 (ApoA1; untreated vs. SKN *P* = 0.022) and of retinol-binding protein 4 (RBP4; untreated vs. SKN *P* = 0.037) and a reduction of platelet-derived growth factor (PDGF) (untreated vs. SKN *P* = 0.021; see Supplementary material online, *Figure S6*). Although not directly related to T-cell activation or metabolism, these data confirm the overall anti-inflammatory effects of the treatments used.

3.5 Oligomycin treatment increases the intra-nuclear translocation of PKM2 and the protein expression of GLUT-1 in HS

To further support the hypothesis of the metabolic loop triggered by PKM2 in NSTEMI patients, we generated a mitochondrial stress condition using OLI[32] in the PBMC culture medium of HS. OLI induced an increase in the nuclear fraction of PKM2 [Manders' tM2, mean ± SD: untreated vs. OLI (*n* = 7) 0.27 ± 0.21 vs. 0.50 ± 0.36; *P* = 0.0074; see Supplementary material online, *Figure S7A and B*] and a resulting enhancement of GLUT-1 [MFI, mean ± SD: Untreated vs. OLI (*n* = 8) 2.686 ± 0.71 vs. 2.821 ± 0.60; *P* = 0.0318] mimicking the PKM2 behaviour in NSTEMI patients (see Supplementary material online, *Figure S7C*).

3.6 Expressions of CD4, GLUT-1, and PKM2 in HCAs and atherosclerotic plaques

In order to better understand the local dysregulation of meta-inflammatory loop, we evaluated the expression of PKM2 and GLUT-1 in HCAs in relation to atherosclerotic plaque presence as well as previous history of CAD (see Supplementary material online, *Table S2*). The results shown in Supplementary material online, *Figure S8* show the haematoxylin and eosin staining and indicate the expressions of CD4, GLUT-1, and PKM2 within the coronary artery sections. As expected, a lymphocyte CD4^{+} infiltrate in coronary section of CAD patients was more evident. Both GLUT-1 and PKM2 were clearly expressed in the coronary artery sections. The expression was particularly evident in the intima of CAD vessels with atherosclerosis, as well as in the core of atherosclerotic plaque itself, providing proof of concept for the local expression of these factors in human atherosclerosis. However, our study was not powered sufficiently to compare quantitative differences between the two studied groups.
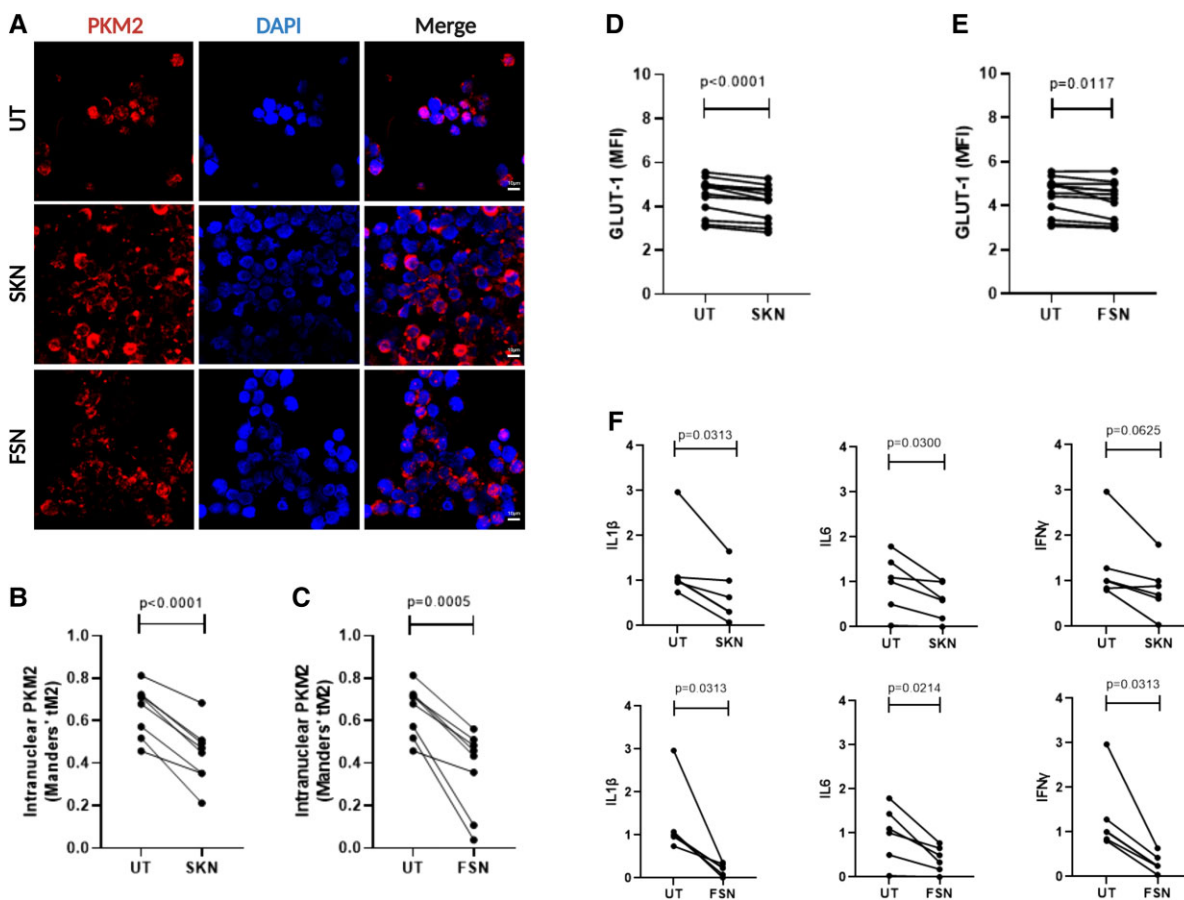
Figure 3 Inhibition of GLUT-1/PKM2 metabolic loop by SKN and FSN in NSTEMI patients. (*A*) Representative immunofluorescence confocal images of PKM2 in the untreated PBMCs and treated with SKN or FSN PBMCs; PKM2 = red fluorescence, nuclei = DAPI; Scale bar: 10 μm for all images; (*B*) intra-nuclear PKM2 level in untreated and SKN-treated PBMCs ($n = 8$); (*C*) intra-nuclear PKM2 level in the untreated and FSN-treated PBMCs ($n = 8$); (*D*) GLUT-1 protein level in the untreated and SKN-treated PBMCs ($n = 12$); (*E*) GLUT-1 protein level in the untreated and FSN-treated PBMCs ($n = 12$); (*F*) inflammatory gene levels in UT-, SKN-, and FSN-treated PBMCs ($n = 5$). In *B*, *C*, *D*, *E*, and *F* (IL-6), for comparisons between groups, we used a paired *t*-test. In *F* (IL-1β and IFNγ), for comparisons between groups, we used a paired samples Wilcoxon test. FSN, fasentin; GLUT-1, glucose transporter 1; IFNγ, interferon gamma; IL-1β, interleukin 1 beta; IL-6, interleukin 6; NSTEMI, non-ST-elevation myocardial infarction; PKM2, pyruvate kinase isozyme M2; SKN, shikonin; UT, untreated.

4. Discussion

4.1 Mechanisms underlying immune-metabolism alteration in NSTEMI

Atherosclerosis is characterized by changes in intracellular metabolic pathways in the arterial wall, including increased glucose uptake, reflecting the degree of vascular inflammation. In an inflammatory setting, immune cells deal with different immune demands dynamically by adapting to various environmental signals and biosynthetic requirements.[33]

As largely demonstrated in previous studies, patients with ACS show an enhanced pro-inflammatory function of effector T cells compared with CCS indicating that the sudden changes, leading to coronary instability, might be related to mechanisms involving dysregulation of adaptive immunity. In the present study, we investigated the role of the two key factors of glucose metabolism, GLUT-1 and PKM2, as potential enhancers of pro-inflammatory response in NSTEMI T cells. Our findings demonstrate that GLUT-1 expression and glucose uptake are increased in stimulated CD4$^+$ T cells in NSTEMI compared with CCS patients and HS, resulting in an increased availability of intracellular glucose which is likely to enhance PKM2 glycolytic activity and the downstream glucose-related pathways. In addition, by dividing patients according to basal glycaemia, hyperglycaemic (HG) CCS patients displayed a higher level of both PKM2 mRNA and protein in comparison with normoglycaemic (NG) CCS, while no significant difference was observed between HG and NG condition in NSTEMI patients. This uncoupling between glycaemia on the one hand and PKM2 mRNA and protein expression on the other suggests that this system is dysregulated in NSTEMI.

More importantly, since PKM2 function depends on its localization, in our study the predominant nuclear localization in NSTEMI probably contributes to increased expression of genes related to glucose metabolism and inflammation and to the enhancement of its transcription level by a mechanism of positive feedback. Accordingly, the functional effects of the disruption of GLUT-1/PKM2 metabolic loop, through SKN and FSN treatment in NSTEMI patients, led to a reduction of PKM2 nuclear translocation accompanied by a decrease of GLUT-1 and the down-regulation of the pro-inflammatory IL-1β, IL-6, and IFNγ gene expression, directly related to T-cell activation. Of note, our data show a deeper down-regulation of pro-inflammatory cytokine genes in samples treated with FSN, a selective inhibitor of GLUT-1, when compared with samples treated with the PKM2 inhibitor SKN. This suggests that other molecular pathways downstream of GLUT-1 other than PKM2 might be involved in the detrimental effect induced by increased glucose levels in NSTEMI patients.

Results from the protein profile on supernatants of treated PBMCs showed the reduction of IL-6 (confirming the down-regulation of IL-6 gene expression), IL-1Ra, MPO, and CHI3L1. While the role of IL-6, IL-1, and MPO in the pathophysiology of ACS has been well elucidated,[34,35] the function of CHI3L1 is poorly understood.[36] Among factors modulated by the GLUT-1/PKM2 pathway, we found an increased level of ApoA1[37–39] and RBP4[40] and a reduction of PDGF after SKN treatment.[41] Although ApoA1 is primarily expressed by the liver and small intestine, it can be also expressed by PBMCs.[38] ApoA1 is the major component of high-density lipoprotein cholesterol, such as, a SKN-mediated increase of ApoA1 could favour the reverse transport of cholesterol.[37,39] In our specific case, the increased levels of ApoA1 protein could be related to the recovery of anti-inflammatory properties following treatments. Although not directly related to T-cell activation or metabolism, these data confirm the overall anti-inflammatory effects of the treatments used.

On the other hand, a mitochondrial stress condition triggered by OLI stimulation, induced a nuclear translocation of PKM2 and a resulting enhancement of GLUT-1 expression in PBMCs of HS.

Although we have not fully elucidated the exact mechanism of PKM2 nuclear translocation in NSTEMI, we suppose that JMJD8, a potential PKM2 negative regulator, is involved in its functional control. In fact, our data show that PKM2 and JMJD8 are mainly co-localized in the T-cell nuclei of CCS compared with NSTEMI patients, suggesting that JMJD8 could act as a limiting factor of the nuclear functions of PKM2.[42]

Taken together, these results highlight the central role of GLUT-1/PKM2 metabolic loop in the meta-inflammation of the NSTEMI patients.

4.2 Study limitations

Our study is exploratory by nature and includes a limited sample size, which is not sufficient to draw a generalizable conclusion about independent clinical predictors; therefore, our findings are to be interpreted as hypothesis generating. We found a higher number of subjects treated with aspirin, beta-blockers, and statins among CCS patients when compared with NSTEMI. Since pharmacological therapy might directly affect T-cell metabolism and activation, we performed a multiple regression analysis, demonstrating that treatment with aspirin, beta-blockers, and statins did not predict glucose uptake [$F(3.52) = 2.13$; $P = 0.11$], GLUT-1 levels [$F(3.62) = 0.62$; $P = 0.61$], and PKM2 levels [$F(3.76) = 0.70$; $P = 0.56$]. Our study lacks of experiments regarding mitochondrial activity and oxidative phosphorylation (OxPHOS); nevertheless, OLI treatments indirectly explore this field. Another limitation of the study is represented by the lack of cell viability assays using specific dyes; however, the combination of FSC and SSC provides a tool, which although not as precise as the fluorescence methods, still gives valuable results in many assays. Indeed, the apoptotic or dying cells can therefore be identified without any staining by FSC and SSC parameters, only by considering the morphology.[43,44] Finally, an ApoE$^{-/-}$ mice model could have the potential to demonstrate the effects of the inhibition of PKM2 nuclear translocation and GLUT-1-related glucose uptake, as mimicked by both SKN and FSN treatments in our mechanistic experiments, on the reduction of atherosclerotic burden and, eventually, infarct size.

4.3 Implications of immune-metabolic dysregulation

Despite the surge in studies on immune metabolism and metabolic reprogramming, only few studies have addressed the role of immune metabolism in atherosclerosis and CAD[14] and, to the best of our knowledge, no study has hitherto investigated immune-metabolic dysregulation in ACS.

New data are emerging on the link between metabolism and epigenetic reprogramming not only in cancer but also in cardiovascular diseases. PKM2 appears to be one of the regulators of metabolism-driven epigenetic modulation and our findings suggest an important role for this molecule in the mechanisms underlying the immune unbalance in NSTEMI patients. Cancer cells express high levels of the monomer and dimeric nuclear forms of PKM2, who stimulate the transcription of various glycolytic genes,

including GLUT-1 and PKM2 itself, with consequent enhancement of glycolysis.[16,27,42] PKM2 plays a central role also in the modulation of the inflammatory state, through the involvement of a pathway related to the signal transducer and activator of transcription 3, stimulating the production of pro-inflammatory cytokines, and regulating the balance between Treg and Th17.[42,45]

Conclusion

Our data propose that aberrant nuclear localization of PKM2 in patients with NSTEMI promotes both the dysregulation of the inflammatory pathways and the increased activation of GLUT-1 and glucose metabolism (Graphical abstract). Therefore, the assessment of the immuno-metabolic profile could help to stratify patients with ACS allowing to identify new therapeutic targets in the perspective of a personalized medicine approach.[46]

Supplementary material

Supplementary material is available at *Cardiovascular Research* online.

Authors' contributions

F.Ca. and D.F. have conceived and designed the study and contributed to data interpretation. F.Ca., D.P., A.S., and R.V. have drafted the manuscript. D.P., A.D.A., M.P., and P.C. have crucially participated in data collection and enrolment of CAD patients. F.Ca., R.V., D.F., E.P., A.Bo., A.D.C., S.R., M.D.S., and G.A. have collected and analysed all the biological parameters. P.S., B.K., and K.W. have contributed with patients' enrolment and collection of the coronary artery samples. P.S., A.Ba., and A.S. have contributed with immunohistochemistry analysis. F.Ca., D.P., A.S., R.V., R.M., D.D.A., T.J.G., G.L., and F.Cr. have revised critically the manuscript for important intellectual content. T.J.G., G.L., and F.Cr. has also given the final approval of the manuscript submitted.

Data availability

The data underlying this article will be shared on reasonable request to the corresponding author.

References

1. Flego D, Liuzzo G, Weyand CM, Crea F. Adaptive immunity dysregulation in acute coronary syndromes: from cellular and molecular basis to clinical implications. *J Am Coll Cardiol* 2016; **68**:2107–2117.

2. Flego D, Severino A, Trotta F, Previtero M, Ucci S, Zara C, Massaro G, Pedicino D, Biasucci LM, Liuzzo G, Crea F. Increased PTPN22 expression and defective CREB activation impair regulatory T-cell differentiation in non-ST-segment elevation acute coronary syndromes. *J Am Coll Cardiol* 2015; **65**:1175–1186.

3. Biasucci LM, La Rosa G, Pedicino D, D'Aiello A, Galli M, Liuzzo G. Where does inflammation fit? *Curr Cardiol Rep* 2017; **19**:84.

4. Angelini G, Flego D, Vinci R, Pedicino D, Trotta F, Ruggio A, Piemontese GP, Galante D, Ponzo M, Biasucci LM, Liuzzo G, Crea F. Matrix metalloproteinase-9 might affect adaptive immunity in non-ST segment elevation acute coronary syndromes by increasing CD31 cleavage on CD4+ T-cells. *Eur Heart J* 2018; **39**:1089–1097.

5. Ruggio A, Pedicino D, Flego D, Vergallo R, Severino A, Lucci C, Niccoli G, Trani C, Burzotta F, Aurigemma C, Leone AM, Buffon A, D'Aiello A, Biasucci LM, Crea F, Liuzzo G. Correlation between CD4(+)CD28(null) T lymphocytes, regulatory T cells and plaque rupture: an optical coherence tomography study in acute coronary syndromes. *Int J Cardiol* 2019; **276**:289–292.

6. Loftus RM, Finlay DK. Immunometabolism: cellular metabolism turns immune regulator. *J Biol Chem* 2016; **291**:1–10.

7. Ramalho R, Rao M, Zhang C, Agrati C, Ippolito G, Wang FS, Zumla A, Maeurer M. Immunometabolism: new insights and lessons from antigen-directed cellular immune responses. *Semin Immunopathol* 2020; **42**:279–313.

8. Pedicino D, Severino A, Ucci S, Bugli F, Flego D, Giglio AF, Trotta F, Ruggio A, Lucci C, Iaconelli A, Paroni Sterbini F, Biasucci LM, Sanguinetti M, Glieca F, Luciani N, Massetti M, Crea F, Liuzzo G. Epicardial adipose tissue microbial colonization and inflammasome activation in acute coronary syndrome. *Int J Cardiol* 2017; **236**:95–99.

9. Palmer CS, Ostrowski M, Balderson B, Christian N, Crowe SM. Glucose metabolism regulates T cell activation, differentiation, and functions. *Front Immunol* 2015; **6**:1–6.

10. Chang CH, Curtis JD, Maggi LB Jr, Faubert B, Villarino AV, O'Sullivan D, Huang SC, van der Windt GJ, Blagih J, Qiu J, Weber JD, Pearce EJ, Jones RG, Pearce EL. Posttranscriptional control of T cell effector function by aerobic glycolysis. *Cell* 2013; **153**:1239–1251.

11. Macintyre AN, Gerriets VA, Nichols AG, Michalek RD, Rudolph MC, Deoliveira D, Anderson SM, Abel ED, Chen BJ, Hale LP, Rathmell JC. The glucose transporter GLUT-1 is selectively essential for CD4 T cell activation and effector function. *Cell Metab* 2014; **20**:61–72.

12. Reckzeh ES, Waldmann H. Small-molecule inhibition of glucose transporters GLUT-1–4. *Chembiochem* 2020; **21**:45–52.

13. Siebeneicher H, Cleve A, Rehwinkel H, Neuhaus R, Heisler I, Müller T, Bauser M, Buchmann B. Identification and optimization of the first highly selective GLUT-1 inhibitor BAY-876. *ChemMedChem* 2016; **11**:2261–2271.

14. Ríos-Silva M, Trujillo X, Trujillo-Hernández B, Sánchez-Pastor E, Urzúa Z, Mancilla E, Huerta M. Effect of chronic administration of forskolin on glycemia and oxidative stress in rats with and without experimental diabetes. *Int J Med Sci* 2014; **11**:448–452.

15. Shirai T, Nazarewicz RR, Wallis BB, Yanes RE, Watanabe R, Hilhorst M, Tian L, Harrison DG, Giacomini JC, Assimes TL, Goronzy JJ, Weyand CM. The glycolytic enzyme PKM2 bridges metabolic and inflammatory dysfunction in coronary artery disease. *J Exp Med* 2016; **213**:337–354.

16. Pan Y, Zheng Q, Ni W, Wei Z, Yu S, Jia Q, Wang M, Wang A, Chen W, Lu Y. Breaking glucose transporter 1/pyruvate kinase M2 glycolytic loop is required for cantharidin inhibition of metastasis in highly metastatic breast cancer. *Front Pharmacol* 2019; **10**:590.

17. Chen J, Xie J, Jiang Z, Wang B, Wang Y, Hu X. Shikonin and its analogs inhibit cancer cell glycolysis by targeting tumor pyruvate kinase-M2. *Oncogene* 2011; **30**:4297–4306.

18. Zhao X, Zhu Y, Hu J, Jiang L, Li L, Jia S, Zen K. Shikonin inhibits tumor growth in mice by suppressing pyruvate kinase M2-mediated aerobic glycolysis. *Sci Rep* 2018; **8**:14517.

19. Yang W, Liu J, Hou L, Chen Q, Liu Y. Shikonin differentially regulates glucose metabolism via PKM2 and HIF1α to overcome apoptosis in a refractory HCC cell line. *Life Sci* 2021; **265**:118796.

20. Wang C, Xiao Y, Lao M, Wang J, Xu S, Li R, Xu X, Kuang Y, Shi M, Zou Y, Wang Q, Liang L, Zheng SG, Xu H. Increased SUMO-activating enzyme SAE1/UBA2 promotes glycolysis and pathogenic behavior of rheumatoid fibroblast-like synoviocytes. *JCI Insight* 2020; **5**:e135935.

21. Tsukada Y, Fang J, Erdjument-Bromage H, Warren ME, Borchers CH, Tempst P, Zhang Y. Histone demethylation by a family of JmjC domain-containing proteins. *Nature* 2006; **439**:811–816.

22. Boeckel JN, Derlet A, Glaser SF, Luczak A, Lucas T, Heumüller AW, Krüger M, Zehendner CM, Kaluza D, Doddaballapur A, Ohtani K, Treguer K, Dimmeler S. JMJD8 regulates angiogenic sprouting and cellular metabolism by interacting with pyruvate kinase M2 in endothelial cells. *Arterioscler Thromb Vasc Biol* 2016; **36**:1425–1433.

23. Collet JP, Thiele H, Barbato E, Barthélémy O, Bauersachs J, Bhatt DL, Dendale P, Dorobantu M, Edvardsen T, Folliguet T, Gale CP, Gilard M, Jobs A, Jüni P, Lambrinou E, Lewis BS, Mehilli J, Meliga E, Merkely B, Mueller C, Roffi M, Rutten FH, Sibbing D, Siontis GCM; ESC Scientific Document Group. 2020 ESC Guidelines for the management of acute coronary syndromes in patients presenting without persistent ST-segment elevation: the task force for the management of acute coronary syndromes in patients presenting without persistent ST-segment elevation of the European Society of Cardiology (ESC). *Eur Heart J* 2021; **42**:1289–1367.

24. Knuuti J, Wijns W, Saraste A, Capodanno D, Barbato E, Funck-Brentano C, Prescott E, Storey RF, Deaton C, Cuisset T, Agewall S, Dickstein K, Edvardsen T, Escaned J, Gersh BJ, Svitil P, Gilard M, Hasdai D, Hatala R, Mahfoud F, Masip J, Muneretto C, Valgimigli M, Achenbach S, Bax JJ; ESC Scientific Document Group. 2019 ESC Guidelines for the diagnosis and management of chronic coronary syndromes: the task force for the diagnosis and management of chronic coronary syndromes of the European Society of Cardiology (ESC). *Eur Heart J* 2020; **41**:407–477.

25. Dang EV, Barbi J, Yang HY, Jinasena D, Yu H, Zheng Y, Bordman Z, Fu J, Kim Y, Yen HR, Luo W, Zeller K, Shimoda L, Topalian SL, Semenza GL, Dang CV, Pardoll DM, Pan F. Control of T(H)17/T(reg) balance by hypoxia-inducible factor 1. *Cell* 2011; **146**:772–784.

26. Liu T, Sun X, Cao Z. Shikonin-induced necroptosis in nasopharyngeal carcinoma cells via ROS overproduction and upregulation of RIPK1/RIPK3/MLKL expression. *Onco Targets Ther* 2019; **12**:2605–2614.

27. Chen L, Shi Y, Liu S, Cao Y, Wang X, Tao Y. PKM2: the thread linking energy metabolism reprogramming with epigenetics in cancer. *Int J Mol Sci* 2014; **15**:11435–11445.

28. Li W, Qu G, Choi SC, Cornaby C, Titov A, Kanda N, Teng X, Wang H, Morel L. Targeting T cell activation and lupus autoimmune phenotypes by inhibiting glucose transporters. *Front Immunol* 2019; **10**:833.

29. Jin X, Zhang W, Wang Y, Liu J, Hao F, Li Y, Tian M, Shu H, Dong J, Feng Y, Wei M. Pyruvate kinase M2 Promotes the activation of dendritic cells by enhancing IL-12p35 expression. *Cell Rep* 2020; **31**:107690.

30. Manders EMM, Verbeek FJ, Aten JA. Measurement of co-localization of objects in dual-colour confocal images. *J Microsc* 1993; **169**:375–382.

31. American Diabetes Association Professional Practice Committee. 2. Classification and diagnosis of diabetes: standards of medical care in diabetes-2022. *Diabetes Care* 2022; **45**:S17–S38.

32. Shin B, Benavides GA, Geng J, Koralov SB, Hu H, Darley-Usmar VM, Harrington LE. Mitochondrial oxidative phosphorylation regulates the fate decision between pathogenic Th17 and regulatory T cells. *Cell Rep* 2020; **30**:1898–1909.e4.

33. Ketelhuth DFJ, Lutgens E, Bäck M, Binder CJ, Van den Bossche J, Daniel C, Dumitriu IE, Hoefer I, Libby P, O'Neill L, Weber C, Evans PC. Immunometabolism and atherosclerosis: perspectives and clinical significance: a position paper from the working group on atherosclerosis and vascular biology of the European society of cardiology. *Cardiovasc Res* 2019; **115**:1385–1392.

34. Biasucci LM, Liuzzo G, Fantuzzi G, Caligiuri G, Rebuzzi AG, Ginnetti F, Dinarello CA, Maseri A. Increasing levels of interleukin (IL)-1Ra and IL-6 during the first 2 days of hospitalization in unstable angina are associated with increased risk of in-hospital coronary events. *Circulation* 1999; **99**:2079–2084.

35. Ferrante G, Nakano M, Prati F, Niccoli G, Mallus MT, Ramazzotti V, Montone RA, Kolodgie FD, Virmani R, Crea F. High levels of systemic myeloperoxidase are associated with coronary plaque erosion in patients with acute coronary syndromes: a clinicopathological study. *Circulation* 2010; **122**:2505–2513.

36. Tsantilas P, Lao S, Wu Z, Eberhard A, Winski G, Vaerst M, Nanda V, Wang Y, Kojima Y, Ye J, Flores A, Jarr KU, Pelisek J, Eckstein HH, Matic L, Hedin U, Tsao PS, Paloschi V, Maegdefessel L, Leeper NJ. Chitinase 3 like 1 is a regulator of smooth muscle cell physiology and atherosclerotic lesion stability. *Cardiovasc Res* 2021; **117**:2767–2780.

37. Zhang Y, Zanotti I, Reilly MP, Glick JM, Rothblat GH, Rader DJ. Overexpression of apolipoprotein A-I promotes reverse transport of cholesterol from macrophages to feces in vivo. *Circulation* 2003; **108**:661–663.

38. Dergunova LV, Nosova EV, Dmitrieva VG, Rozhkova AV, Bazaeva EV, Limborska SA, Dergunov AD. HDL cholesterol is associated with PBMC expression of genes involved in HDL metabolism and atherogenesis. *J Med Biochem* 2020; **39**:372–383.

39. Busnelli M, Manzini S, Colombo A, Franchi E, Bonacina F, Chiara M, Arnaboldi F, Donetti E, Ambrogi F, Oleari R, Lettieri A, Horner D, Scanziani E, Norata GD, Chiesa G. Lack of ApoA-I in ApoEKO mice causes skin xanthomas, worsening of inflammation, and increased coronary atherosclerosis in the absence of hyperlipidemia. *Arterioscler Thromb Vasc Biol* 2022; **42**:839–856.

40. Olsen T, Blomhoff R. Retinol, retinoic acid, and retinol-binding protein 4 are differentially associated with cardiovascular disease, type 2 diabetes, and obesity: an overview of human studies. *Adv Nutr* 2020; **11**:644–666.

41. Zhang H, Zhang Y, Liu Y, Ma K, Zhou J, Guan J. Platelet-derived growth factor predicts vulnerable plaque in patients with non-st elevation acute coronary syndrome. *Am J Med Sci* 2021; **361**:759–764.

42. Koo SJ, Garg NJ. Metabolic programming of macrophage functions and pathogens control. *Redox Biol* 2019; **24**:101198.

43. Cossarizza A, Chang HD, Radbruch A, ACS A, Adam D, Adam-Klages S, Agace WW, Aghaeepour N, Akdis M, Allez M, Almeida LN, Alvisi G, Anderson G, Andrä I, Annunziato F, Anselmo A, Bacher P, Baldari CT, Bari S, Barnaba V, Barros-Martins J, Battistini L, Bauer W, Baumgart S, Baumgart N, Baumjohann D, Baying B, Bebawy M, Becher B, Beisker W, Benes V, Beyaert R, Blanco A, Boardman DA, Bogdan C, Borger JG, Borsellino G, Boulais PE, Bradford JA, Brenner D, Brinkman RR, Brooks AES, Busch DH, Büscher M, Bushnell TP, Calzetti F, Cameron G, Cammarata MA, Cao X, Cardell SL, Casola S, Cassatella MA, Cavani A, Celada A, Chatenoud L, Chattopadhyay PK, Chow S, Christakou E, Čičin-Šain L, Clerici M, Colombo FS, Cook L, Cooke A, Cooper AM, Corbett AJ, Cosma A, Cosmi L, Coulie PG, Cumano A, Cvetkovic L, Dang VD, Dang-Heine C, Davey MS, Davies D, De Biasi S, Del Zotto G, Dela Cruz GV, Delacher M, Della Bella S, Dellabona P, Deniz G, Dessing M, Di Santo JP, Diefenbach A, Dieli F, Dolf A, Dörner T, Dress RJ, Dudziak D, Dustin M, Dutertre CA, Ebner F, Eckle SBG, Edinger M, Eede P, Ehrhardt GRA, Eich M, Engel P, Engelhardt B, Erdei A, Esser C, Everts B, Evrard M,

Falk CS, Fehniger TA, Felipo-Benavent M, Ferry H, Feuerer M, Filby A, Filkor K, Fillatreau S, Follo M, Förster I, Foster J, Foulds GA, Frehse B, Frenette PS, Frischbutter S, Fritzsche W, Galbraith DW, Gangaev A, Garbi N, Gaudilliere B, Gazzinelli RT, Geginat J, Gerner W, Gherardin NA, Ghoreschi K, Gibellini L, Ginhoux F, Goda K, Godfrey DI, Goettlinger C, González-Navajas JM, Goodyear CS, Gori A, Grogan JL, Grummitt D, Grützkau A, Haftmann C, Hahn J, Hammad H, Hämmerling G, Hansmann L, Hansson G, Harpur CM, Hartmann S, Hauser A, Hauser AE, Haviland DL, Hedley D, Hernández DC, Herrera G, Herrmann M, Hess C, Höfer T, Hoffmann P, Hogquist K, Holland T, Höllt T, Holmdahl R, Hombrink P, Houston JP, Hoyer BF, Huang B, Huang FP, Huber JE, Huehn J, Hundemer M, Hunter CA, Hwang WYK, Iannone A, Ingelfinger F, Ivison SM, Jäck HM, Jani PK, Jávega B, Jonjic S, Kaiser T, Kalina T, Kamradt T, Kaufmann SHE, Keller B, Ketelaars SLC, Khalilnezhad A, Khan S, Kisielow J, Klenerman P, Knopf J, Koay HF, Kobow K, Kolls JK, Kong WT, Kopf M, Korn T, Kriegsmann K, Kristyanto H, Kroneis T, Krueger A, Kühne J, Kukat C, Kunkel D, Kunze-Schumacher H, Kurosaki T, Kurts C, Kvistborg P, Kwok I, Landry J, Lantz O, Lanuti P, LaRosa F, Lehuen A, LeibundGut-Landmann S, Leipold MD, Leung LYT, Levings MK, Lino AC, Liotta F, Litwin V, Liu Y, Ljunggren HG, Lohoff M, Lombardi G, Lopez L, López-Botet M, Lovett-Racke AE, Lubberts E, Luche H, Ludewig B, Lugli E, Lunemann S, Maecker HT, Maggi L, Maguire O, Mair F, Mair KH, Mantovani A, Manz RA, Marshall AJ, Martínez-Romero A, Martrus G, Marventano I, Maslinski W, Matarese G, Mattioli AV, Maueröder C, Mazzoni A, McCluskey J, McGrath M, McGuire HM, McInnes IB, Mei Melchers F, Melzer S, Mielenz D, Miller SD, Mills KHG, Minderman H, Mjösberg J, Moore J, Moran B, Moretta L, Mosmann TR, Müller S, Multhoff G, Muñoz LE, Münz C, Nakayama T, Nasi M, Neumann K, Ng LG, Niedobitek A, Nourshargh S, Núñez G, O'Connor JE, Ochel A, Oja A, Ordonez D, Orfao A, Orlowski-Oliver E, Ouyang W, Oxenius A, Palankar R, Panse I, Pattanapanyasat K, Paulsen M, Pavlinic D, Penter L, Peterson P, Peth C, Petriz J, Piancone Pickl WF, Piconese S, Pinti M, Pockley AG, Podolska MJ, Poon Z, Pracht K, Prinz I, Pucillo CEM, Quataert SA, Quatrini L, Quinn KM, Radbruch H, Radstake TRDJ, Rahmig S, Rahn HP, Rajwa B, Ravichandran G, Raz Y, Rebhahn JA, Recktenwald D, Reimer D, Reis e Sousa C, Remmerswaal EBM, Richter L, Rico LG, Riddell A, Rieger AM, Robinson JP, Romagnani C, Rubartelli A, Ruland J, Saalmüller A, Saeys Y, Saito T, Sakaguchi S, Sala-de-Oyanguren F, Samstag Y, Sanderson S, Sandrock I, Santoni A, Sanz RB, Saresella M, Sautes-Fridman C, Sawitzki B, Schadt L, Scheffold A, Scherer HU, Schiemann M, Schildberg FA, Schimisky E, Schlitzer A, Schlosser J, Schmid S, Schmitt S, Schober K, Schraivogel D, Schüler T, Schulte R, Schulz AR, Schulz SR, Scottá C, Scott-Algara D, Sester DP, Shankey TV, Silva-Santos B, Simon AK, Sitnik KM, Sozzani S, Speiser DE, Spidlen J, Stahlberg A, Stall AM, Stanley N, Stark R, Stehle C, Steinmetz T, Stockinger H, Takahama Y, Takeda K, Tan L, Tárnok A, Tiegs G, Toldi G, Tornack J, Traggiai E, Trebak M, Tree TIM, Trotter J, Trowsdale J, Tsoumakidou M, Ulrich H, Urbanczyk S, van de Veen W, van den Broek M, van der Pol E, Van Gassen S, Van Isterdael G, van Lier RAW, Veldhoen M, Vento-Asturias S, Vieira P, Voehringer D, Volk HD, von Borstel A, von Volkmann K, Waisman A, Walker RV, Wallace PK, Wang SA, Wang XM, Ward MD, Ward-Hartstonge KA, Warnatz K, Warnes G, Warth S, Waskow C, Watson JV, Watzl C, Wegener L, Weisenburger T, Wiedemann Wienands J, Wilharm A, Wilkinson RJ, Willimsky G, Wing JB, Winkelmann R, Winkler TH, Wirz OF, Wong A, Wurst P, Yang JHM, Yang J, Yazdanbakhsh M, Yu L, Yue A, Zhang H, Zhao Y, Ziegler SM, Zielinski C, Zimmermann J, Zychlinsky A . Guidelines for the use of flow cytometry and cell sorting in immunological studies (second edition). *Eur J Immunol* 2019;**49**:1457–1973.

44. Reardon AJ, Elliott JA, McGann LE. Fluorescence as an alternative to light-scatter gating strategies to identify frozen-thawed cells with flow cytometry. *Cryobiology* 2014;**69**: 91–99.

45. Zhang Z, Deng X, Liu Y, Liu Y, Sun L, Chen F. PKM2, function and expression and regulation. *Cell Biosci* 2019;**9**:52.

46. Bona RD, Liuzzo G, Pedicino D, Crea F. Anti-inflammatory treatment of acute coronary syndromes. *Curr Pharm Des* 2011;**17**:4172–4189.

Translational perspective

This study investigates the role of glucose metabolism and the key glycolytic enzyme PKM2 on adaptive immunity dysregulation in patients with the acute coronary syndrome, leading to a better understanding of the role of meta-inflammation in coronary plaque instability. Our study paves the way to a more accurate patient's stratification, based on immune-metabolic features, and to the detection of novel molecular biomarkers that could become, with further validating studies, promising pharmacological targets, in the perspective of a personalized medicine approach.